Cell. Mol. Life Sci. (2015) 72:3375–3385
DOI 10.1007/s00018-015-1893-3

Cellular and Molecular Life Sciences

RESEARCH ARTICLE

Mutations of the SL2 dimerization sequence of the hepatitis C genome abrogate viral replication

Cyril Masante[1,2] · Chloé Jaubert[1,2] · William Palau[3,4] · Jacqueline Plissonneau[1,2] · Lucie Besnard[1,2] · Michel Ventura[1,2] · Carmelo Di Primo[3,4]

Received: 17 December 2014 / Revised: 3 March 2015 / Accepted: 20 March 2015 / Published online: 28 March 2015

Abstract Stem-loop SL2 is a self-interacting palindromic sequence that has been identified within the hepatitis C virus genome (HCV). While, RNA dimerization of the HCV genome has been observed in vitro with short RNA sequences, the role of a putative RNA dimerization during viral replication has not been elucidated. To determine the effect of genomic dimerization on viral replication, we introduced mutations into SL2 predicted to disrupt genomic dimerization. Using surface plasmon resonance, we show that mutations within the SL2 bulge impact dimerization in vitro. Transfection of Huh7 cells with luciferase-encoding full-length genomes containing SL2 mutations abolishes viral replication. Luciferase expression indicates that viral translation is not or slightly affected and that the viral RNA is properly encapsidated. However, RT-qPCR analysis demonstrates that viral RNA synthesis is drastically decreased. In vitro synthesis experiments using the viral recombinant polymerase show that modifications of intra-molecular interactions have no effect on RNA synthesis, while impairing inter-molecular interactions decreases polymerase activity. This confirms that dimeric templates are preferentially replicated by the viral polymerase. Altogether, these results indicate that the dimerization of the HCV genomic RNA is a crucial step for the viral life cycle especially for RNA replication. RNA dimerization could explain the existence of HCV recombinants in cell culture and patients reported recently in other studies.

Keywords Genome dimerization · Viral replication · RNA-dependent RNA polymerase · Structured RNA · Surface plasmon resonance

C. Masante and C. Jaubert are the joint first authors.

M. Ventura and C. Di Primo contributed equally to this work.

✉ Michel Ventura
michel.ventura@u-bordeaux.fr

✉ Carmelo Di Primo
carmelo.diprimo@inserm.fr

[1] Univ. Bordeaux, Laboratoire MFP, 33076 Bordeaux, France

[2] CNRS UMR 5234, Laboratoire MFP, 33076 Bordeaux, France

[3] Univ. Bordeaux, Laboratoire ARNA, 33076 Bordeaux, France

[4] INSERM, U869, Laboratoire ARNA, 33607 Pessac, France

Introduction

The genome of hepatitis C virus (HCV), a member of the family *Flaviviridae*, contains several intra-molecular structures that are important for many viral processes. Similar to other RNA viruses, disruption of these critical structures can significantly impair virus replication. Research over the past years has demonstrated that interactions within and between the 5′ and 3′ termini of the HCV genome are essential for efficient viral replication [1]. Results obtained by RNA mapping [2–4] and by reverse genetics [5–7] have provided much insight into the function of these genomic structures across the 9600 nt HCV genome. The positive-polarity viral RNA is composed of a large open reading frame flanked by 5′ and 3′ untranslated regions (UTRs). The 5′UTR encompasses the internal ribosomal entry site (IRES), a highly structured region of RNA that ensures translation of the viral polyprotein. The 5′UTR interacts with domain VI of the core coding sequence to form a pseudoknot [8] that is thought to regulate

the efficiency of cap-independent translation. The 3′UTR is composed of 98 invariant nucleotides that fold as three stem-loops (SL): SL1 to SL3. Structures within both the 5′ and 3′UTRs have also been demonstrated to interact with more distal elements of the HCV genome [1]. The 5BSL3.2 structure, located at the 3′ end of the NS5B gene, is a central element capable of interacting with SL2 through loop–loop recognition. Also, this region is capable of interacting with domain IIId of the 5′UTR [9] and an upstream sequence located on the NS5B gene [5].

Inter-molecular interactions are also important during the replication of several RNA viruses. Genomic dimerization is essential for genome packaging and infectivity for members of the *Retroviridae* family [10, 11]. Genome dimerization is also involved in the ribosomal frameshift that occurs during severe acute respiratory syndrome coronavirus (SARS-CoV) replication [12]. For HCV, genomic dimerization has been described in vitro in the presence of the core protein [13–15]. It was shown to be mediated by a palindromic sequence located on the 5′ side of SL2 [16]. This RNA–RNA interaction is triggered by a kissing loop interaction between two structurally rearranged SL2s [17]. While the HCV core protein is required in some experimental conditions, we showed recently, using surface plasmon resonance (SPR), that one conformation of SL2 is capable of dimerization in the absence of any protein [18]. Recent studies using reporter constructs [3] and SHAPE analysis with the full-length J6/JFH1 genomic RNA [4], provide further support that the palindromic sequence on the 5′ side of SL2 is important for this RNA–RNA interaction. Despite the genetic variability of HCV, this 16-nt-long palindromic sequence within SL2 is conserved in all HCV isolates, suggesting that genomic dimerization could be important during virus replication.

Though the HCV virion is thought to contain only one RNA molecule, genomic dimerization could conceivably function in genomic recombination and/or packaging. Recombination events are well known in lentiviruses such as human immunodeficiency virus (HIV). The mechanisms driving recombination have been investigated extensively. It involves dimerization of the genomic RNA followed by jumping of the reverse transcriptase between the two plus strands. Numerous studies with *Retroviridae* family members have established that packaging of the viral genome and retro-transcription are dependent upon this dimerization stage [10, 11]. For HCV, recombinant strains have been reported in infected patients [19, 20], and in vitro recombination events have been recently described [21]. Though rare [22], such events would likely require both genomes to be in close proximity, potentially through SL2 interactions.

In this study, we investigated whether mutations that prevent dimerization of SL2 affect viral replication by measuring virus translation and replication levels, and by determining the effect on RNA-dependent RNA polymerase (RdRp) activity. Our data indicate that dimerization of the HCV genomic RNA is a crucial step during the viral life cycle and that dimeric RNA substrate is required for an efficient RdRp activity.

Materials and methods

Oligonucleotides

RNA oligonucleotides were purchased from Dharmacon (GE Healthcare Europe GmbH, Vélizy-Villacoublay, France) purified by electrophoresis in 7 M urea 20 % polyacrylamide gels, and desalted on Sephadex G-25 spin columns prepared in 1 mL syringes. The secondary structure predictions were performed using the Mfold web server at http://mfold.rna.albany.edu/?q=node/60 [23].

Plasmids and vectors

The pGEM-T/5UTR-H2AE-5BSL-3UTR vector was constructed from the previously described pGEM-T/5UTR-H2AE-3UTR vector [24] by inserting the last 275 nt of the HCV NS5B gene between the EGFP stop codon and the 3′UTR. The JFH-1 backbone was modified by introducing 99 silent mutations into E1, 6 mutations into E2, and by inserting 18 nt into the NS5A gene at position 7523. The resulting whole HCV genome (LMTV: Genbank HG948568) was obtained by gene synthesis (Eurofins MWG/Operon, Ebersberg, Germany) and cloned into pUC19. The gene encoding Gaussia luciferase (GLuc) ending in 60 nt that coded for the FMDV 2A protein, was obtained by gene synthesis and was further introduced between the p7 and NS2 genes at position 2779. Mutations in the SL2 stem (kistem and TD, Fig. 1) were obtained by gene synthesis and cloned between the EcoR*V* and Xba*I* sites in the pUC/LMTV-Gluc vector and between the BssH*II* and Sph*I* sites in the pGEM-T/5UTR-H2AE-5BSL-3UTR vector. The 5BSL3.2 apical and SL2 apical loops were mutated using site-directed mutagenesis by exchanging TCAC with AAAG in 5BSL3.2, and GTGA with CCTT in SL2 of the pGEM-T/5UTR-H2AE-5BSL-3UTR vector.

In vitro transcription

The template for producing the LMTV genomic RNA was obtained by cleavage of the XbaI site of pUC/LMTV-Gluc. The templates used for in vitro transcription to produce the 5UTR-H2AE-5BSL-3UTR RNAs and the WT555, TD555

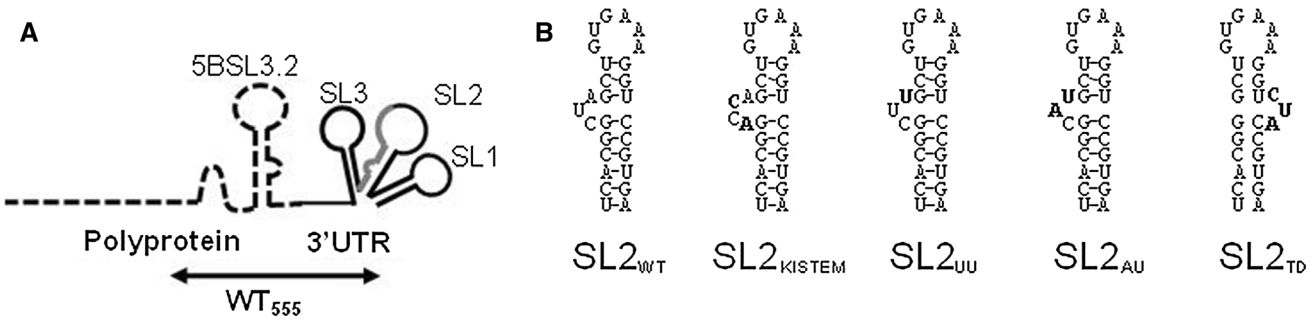

Fig. 1 Schematics of: **A** the RNA 3′ end and **B** the SL2 mutants

Table 1 List of primers

Primer	Sequence 5′→3′
T7_5UTR_Start	TAATACGACTCACTATAGGGCCAG CCCCCGATTGGGGGCGACAC
T7_555_Start	TAATACGACTCACTATAGGGCATGGA CGACTGTACAAGTAATC
3UTR_Stop	ACTTGATCTGCAGAGAGGCCAG
NS3_S	AAGTCTTTGGAGCCGTGCAA
NS3_AS	TGTCTCAACGGGGATGAAAT
EGFP_S	GACCACATGAAGCAGCACGA
EGFP_AS	GACGTTGTGGCTGTTGTAGT
SFRS4_S	AAAAGTCGGAGCAGGAGTCA
SFRS4_AS	CTCTTCCTGCCCTTCCTCTT

and Kistem555 RNAs were obtained using PCR with primers T7_5UTR_Start or T7_555_Start and 3UTR_Stop, which were designed to introduce a T7 RNA polymerase promoter (Table 1). PCR and in vitro transcription have been described previously [25], and the purity and integrity of the RNAs were determined using capillary electrophoresis on a Bioanalyzer 2100 (Agilent).

Surface plasmon resonance experiments

SPR experiments were performed at 10 °C using a Biacore™ T200 (Biacore™, GE Healthcare Lifesciences, Upsala, Sweden). A HC200 m sensor chip (XantecBioanalytics, Düsseldorf, Germany) was coated with 5000 resonance units (RU) of streptavidin (Roche Applied Sciences, Meylan, France) using the Biacore™ amine-coupling kit. 5′ biotinylated RNAs (150 RU) were immobilized on one flow cell. One blank flow cell was used for double-referencing of the sensorgrams using BiaEval 4.1 (Biacore™). The RNA samples injected over the functionalized surface, prepared in running buffer (10 mM sodium phosphate buffer, pH 7.2 at 20 °C, 50 mM NaCl, 3 mM $MgCl_2$, 0.05 % Tween-20), were heated for 1 min and 30 s at 90 °C, and then put on ice for 5 min. The samples were injected at 50 µL/min. The regeneration of the surface was achieved using a 2-min pulse of a mixture of 40 % formamide, 3.6 M urea and 30 mM EDTA, prepared in Milli-Q water [26].

Native gels and staining of RNA oligonucleotides

Native gels were prepared using 15 % (w/v) 75:1 acrylamide/bis (acrylamide) in 50 mM Tris–acetate buffer, pH 7.3 at 20 °C, 3 mM magnesium acetate (migration buffer). Two micrograms of RNA were heated for 1 min and 30 s at 90 °C, and then put on ice for 5 min. Electrophoresis was conducted at 300 V for 3 h after gel equilibration at 10 °C. The gels were stained for 30 min in the dark using the "Stainsall" dye (Acros Organics).

Cell culture and transient RNA transfection

All cell lines were cultured in Dulbecco's modified Eagle medium supplemented with 10 % fetal calf serum and gentamycin (50 µg/mL) at 37 °C in a 5 % CO_2 atmosphere. The Huh7-QR cells were obtained from cell line harboring the Rep5.1 RNA replicon (kindly provided by R. Bartenschlager). These cells were cured by a three-week treatment with 150 U/mL interferon-α until disappearance of the replicon RNA [25].

Transient transfections were performed by seeding 24- or 96-well plates with 8×10^4 or 2×10^4 of the appropriate cells, respectively. For the 24-well plates, cells were seeded 24 h before transfection, and each RNA transfection point was performed using 1 µg of RNA combined with 3 µL of the transfection agent DMRIE-C, according to the manufacturer's instructions (Invitrogen). For the 96-well plates, cells were seeded with 300 ng of RNA combined with 0.6 µL of DMRIE-C. The fluorescence intensity was measured using flow cytometry (Beckton-Dickinson, LSR Fortessa), and GLuc activity from 4 µL of viral supernatant diluted in 1 µL of lysis buffer (Luciferase Cell Lysis Buffer, BioLabs) was measured using the BioLuxGLuc Substrate (BioLabs) and the VariosKan apparatus (ThermoScientific).

RNA isolation

Total RNA was extracted using TRI-Reagent (Molecular Research Center, Inc.). Viral RNA was extracted from 250 µL of culture supernatant using TRIzol-LS (Life Technologies), according to the manufacturer's instructions and then resuspended in 50 µL of H_2O.

Quantitative RT-PCR

The NS3_S and NS3_AS primers (Table 1) were designed to amplify a portion of the NS3 region of the HCV LMTV RNA. EGFP_S and EGFP_AS (Table 1) were designed to amplify a portion of the EGFP gene. The HCV RNA copy number was normalized to the SFRS4 cellular RNA, which is relatively stable in HCV-infected cells [25, 27]. The SFRS4_S and SFRS4_AS primers (Table 1) were used. Reactions were performed as described previously [25]. The copy numbers of NS3, EGFP and SFRS4 were determined by comparison with specific, serially diluted transcripts that were included in the RT-PCR analysis. To avoid the effect of potential inhibitors in the extract, RT-qPCR reactions were performed on 5 µL of three dilutions of cellular RNA. The copy number was calculated as the average of the triplicates after applying the dilution factor.

RdRp assays

Recombinant HCV NS5B-delta21 was expressed in *Escherichia coli,* purified as described previously [28] and used in all experiments. The assay was performed for 2 h at 30 °C as previously described [29] with 40 nM RNA templates and 320 nM purified NS5B.

Results

Design and analysis of dimerization mutants

Before testing whether HCV genomic dimerization was important during the HCV life cycle, we first analyzed in vitro SL2 mutants to ensure that only dimerization was disrupted [7], and not other interactions involving SL2. This sequence was shown to fold as two major secondary structures [15]. One of them displays an apical loop partially complementary to the apical loop of 5BSL3.2, a stem-loop located upstream. The RNA structure was proposed to be a molecular hub that could control the destiny of the viral RNA [15]. Because the interaction between SL2 and 5BSL3.2 occurs through loop–loop recognition [6], we only mutated the nucleotides located in the SL2 bulge, i.e., in the dimer linkage sequence (DLS). This palindromic sequence was shown to be responsible for the dimerization in vitro of short RNA sequences at the 3′ end of the HCV genome. The $SL2_{kistem}$ mutant (Fig. 1B) was designed to stabilize the SL2 conformation that interacts with 5BSL3.2. Previous work has shown that this mutant impairs dimer formation by sequestering the nucleotides of the DLS in the stem [18]. $SL2_{UU}$ and $SL2_{AU}$ (Fig. 1B) was designed to prevent the formation of the kissing complex that would trigger dimer formation according to Shetty et al. [17]. An additional mutant expected to prevent dimerization, $SL2_{TD}$ (Fig. 1B), was designed by translocating the bulge from the 5′ to the 3′ side of the stem. The wild type ($SL2_{WT}$) and mutant SL2 sequences were synthesized with a 5′ biotin tag to allow immobilization on streptavidin-coated sensor chips. A truncated version of 5BSL3.2 that displays the minimal structural motif capable of interacting with SL2, mini5BSL3.2 [18], was used as a control, to test whether these SL2 structures could still interact with 5BSL3.2.

We first analyzed the self-association of the SL2 mutants by SPR (Fig. 2A) and electrophoresis on native polyacrylamide gels (Fig. 2B). $SL2_{WT}$ and mini5BSL3.2 were first injected over $SL2_{WT}$ that was immobilized on the sensor chip surface (Fig. 2A, a). The observed increase in SPR signals demonstrates that $SL2_{WT}$ interacts with both itself and mini5BSL3.2, which is in perfect agreement with our previous work (Palau et al. 2013). The sensorgrams obtained when mini5BSL3.2 was injected against the SL2 mutants (Fig. 2A, b–e) show that the four mutants still interact with 5BSL3.2. The results show that $SL2_{AU}$ clearly dimerized (Fig. 2A, d), but $SL2_{kistem}$, $SL2_{UU}$ and $SL2_{TD}$ could not self-associate (Fig. 2A, b, c, e). To support these results, the four SL2 mutants were analyzed on native polyacrylamide gels (Fig. 2B). Two major bands were observed for $SL2_{WT}$ and $SL2_{AU}$, consistent with the dimerization observed by SPR experiments. However, only a single band was observed for $SL2_{kistem}$ and $SL2_{TD}$ corroborating the results obtained by SPR. The single band observed for $SL2_{UU}$, migrated more slowly compared to $SL2_{kistem}$ and $SL2_{TD}$, suggesting that $SL2_{UU}$ adopts a different monomeric conformation than the other SL2 constructs. Because of that, the $SL2_{UU}$ mutant was not considered for further experiments. Only the $SL2_{kistem}$ and $SL2_{TD}$ mutants were introduced in the genomic constructs to investigate the biological effects of the dimerization observed in vitro. These SL2 structures unable to self-associate, retain the capacity to interact with mini5BSL3.2.

RNA genomic dimerization is required for viral replication

To examine the impact of genomic dimerization during HCV replication, the mutations generating the $SL2_{kistem}$

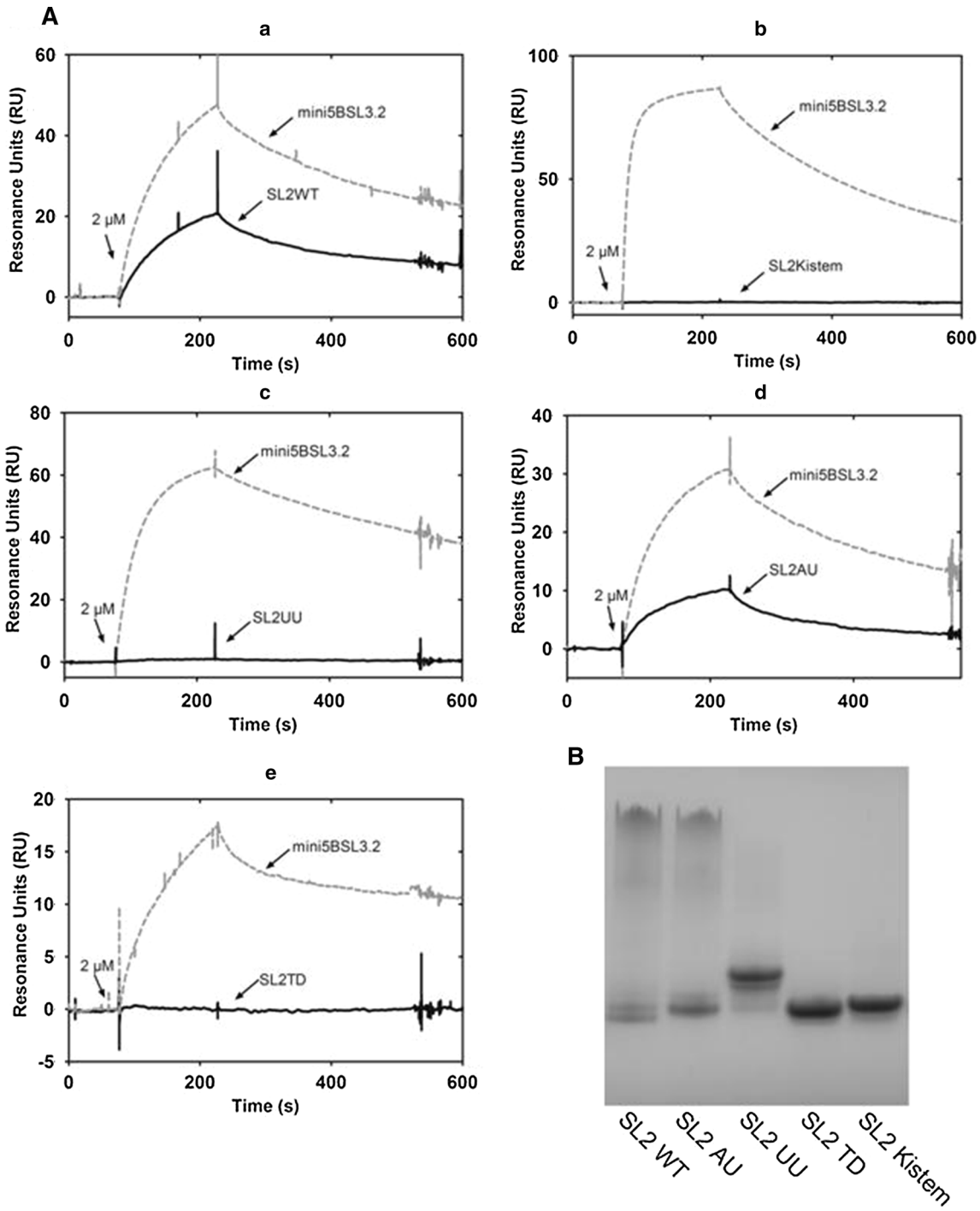

Fig. 2 Selection of dimerization mutants. **A** Kinetic analysis of SL2 binding to itself. The homolog mutants and the truncated version of 5BSL3.2, mini5BSL3.2, were injected over SL2 at 2 µM for 150 s, as indicated by the *arrows*. **a** $SL2_{WT}$, **b** $SL2_{kistem}$, **c** $SL2_{UU}$, **d** $SL2_{AU}$, **e** $SL2_{TD}$ **B** Native polyacrylamide gel electrophoresis of the SL2 hairpins. Two micrograms of $SL2_{AU}$, $SL2_{WT}$, $SL2_{kistem}$, $SL2_{UU}$ and $SL2_{TD}$ was prepared and loaded onto 15 % (w/v) 75:1 acrylamide/bis (acrylamide) native gels. *XC* xylene cyanol

and $SL2_{TD}$ secondary structures were inserted into the LMTV-Gluc virus. None of these mutations disrupted the interaction between the apical loop of 5BSL3.2 and the SL2 loop according to our SPR experiments. Viruses produced by gene synthesis contained 115 silent mutations across the E1 and E2 genes of the JFH-1 backbone. GLuc was fused to the FMDV 2A protein gene and inserted between p7 and NS2. The replication level of LMTV-GLuc was similar to that of the JFH-1 parental strain (data not shown).

We analyzed the effects of these SL2 mutations on virus replication by transfecting Huh7-QR cells with each viral RNA. The wild type viral RNA efficiently produced the GLuc protein 24 h post-transfection, and the signal increased exponentially between 48 and 72 h indicative of actively replicating virus (Fig. 3A). In contrast, no time-dependent increase in GLuc activity was observed for LMTV-GLuc$_{Kistem}$ and LMTV-GLuc$_{TD}$ RNA following transfection. The level of GLuc expressed by LMTV-GLuc$_{Kistem}$ and LMTV-GLuc$_{TD}$ at 24 h indicates that GLuc was translated equally to the wild type virus following transfection but that mutant viruses was not actively replicating.

To confirm our GLuc studies and to determine which step of virus replication was impaired, we analyzed virus production by using RT-qPCR. Huh7 cells were split 72 h post-transfection and cultured for three days to eliminate the transfected RNA and to allow sufficient time for virus replication (Fig. 3B, plating 1). A second passage was performed 72 h after the first one and the cells were cultured for an additional three days. Both intracellular and supernatant viral RNA levels were quantified by RT-qPCR before each passage (Fig. 3B, plating 2). If the mutations within SL2 affect RNA replication, the number of intracellular and supernatant viral genomes should decrease. However, if encapsidation is hindered, the number of viral genomes should decrease only in the supernatant, while intracellular RNA should remain unchanged. For the wild type virus, the number of intracellular viral genomes remained similar between first and the second passages (46 ± 10 versus 47 ± 11 HCV copies/Sfrs4 copy). In contrast, a decrease in the number of viral genomes present within the supernatant was observed ($24 \times 10^3 \pm 7 \times 10^3$ versus $5 \times 10^3 \pm 1 \times 10^3$ copies/μL). For the SL2 mutant viruses, the number of intracellular viral genomes was decreased following the first passage, however, viral RNA levels in the supernatant were unchanged (Fig. 3B, plating 1). This suggests that the input genomes were competent for translation and were still efficiently encapsidated. Following passage two, no intracellular viral genome was detected and viral RNA levels in the supernatant were almost completely abolished (Fig. 3B, plating 2). To confirm that encapsidation was unaffected, we infected naïve Huh7 cells with viral supernatant harvested 72 h post-

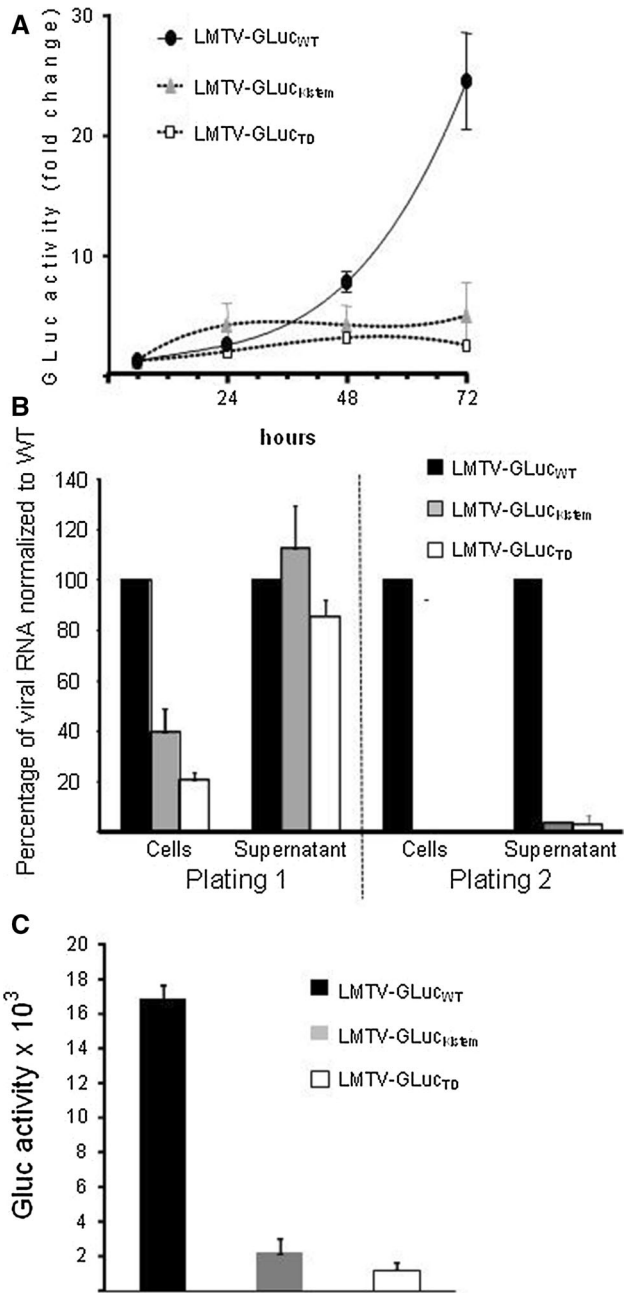

Fig. 3 Effect of SL2 bulge mutations on viral replication. One microgram of LMTV-GLuc$_{WT}$ (*black*), LMTV-GLuc$_{Kistem}$ (*dark grey*) or LMTV-GLuc$_{TD}$ (*light grey*) was transfected into 10^5 Huh7-QR cells that were plated the day before into 24-well plates using DMRIE-C. **A** GLuc expression was measured in 4 μL of culture supernatant at 24, 48 and 72 h post-transfection ($n = 3$ representative experiments in duplicate/Error bars, mean ± SEM). **B** Seventy-two hours post-transfection, cells that were transfected with the 3 viruses were split 1/3. Three days later, each cell line was split again at 1/3, or RNAs were extracted from the cells and supernatant using TRI-Reagent or TRIzol-LS, respectively. Another three days later, at the second passage, RNAs were extracted from cells and supernatant as described above. Genomic RNA in the cell extract and supernatant was quantified by RT-qPCR of the NS3 gene using SFRS4 RNA as the control for cellular RNAs. The results were normalized to 100 for the LMTV-GLuc$_{WT}$ ($n = 3$ independent experiments/error bars, mean ± SEM using 2 different RNA preparations). **C** Seventy-two hours post-transfection, cells transfected by the 3 viruses were split 1/3 into new wells, and after 3 days of culture, 50 μL of each viral supernatant was used to infect 10^5 naïve Huh7-QR cells. After 48 h, the GLuc expression was measured as described above ($n = 3$ independent experiments in duplicate/*error bars*, mean ± SEM using 2 different RNA preparations)

transfection. Consistent with our RT-qPCR data, wild type virus exhibited high luciferase activity following infection (Fig. 3C). All of the SL2 mutants produced very low levels of luciferase activity (Fig. 3C) despite high levels of RNA within the supernatant (Fig. 3B), demonstrating that these particles are capable of entering Huh7 cells, but are replication incompetent. Taken together, these results indicate that mutations within SL2 do not affect virus entry, genome translation, or encapsidation, but significantly impair genomic replication.

Effect of RNA genomic dimerization at the translation level

While our data show that SL2 mutations directly impact genome replication, this could also be due to poor translation of non-structural proteins (NS) or altered RdRp activity following virus entry. To test this, we analyzed the effects of SL2 mutations on translation using RNA constructs expressing EGFP. The 5′ end of the EGFP coding sequence was fusioned to the HCV 5′UTR to ensure efficient translation, while the 3′ end was fused to the last 275 nt of NS5B and the HCV 3′UTR. The presence of these 5′ and 3′ sequences recapitulates the RNA–RNA interactions that were described recently within the viral genome (Fig. 4A). Mutations preventing genomic dimerization were introduced into this construct, named 5UTR-H2AE-5BSL-3UTR. This RNA was transfected into Huh7-QR cells, and translation was assayed using flow cytometry 24 h post-transfection. Clear decreases in EGFP synthesis were observed for the mutant RNAs (Fig. 4B), as compared to the wild type. The two mutants, 5UTR-H2AE-5BSL-3UTR$_{Kistem}$ and 5UTR-H2AE-5BSL-3UTR$_{TD}$, produced nearly twofold less EGFP than the wild type construct, 56 ± 8 % and 52 ± 5 %, respectively.

Because the level of EGFP synthesis is dependent on RNA stability, we also measured the decrease of RNA constructs as a function of time. The RNA was isolated 24 and 72 h post-transfection and the amount of EGFP was quantified using RT-qPCR. The RNA quantification was normalized to the wild type construct, which was assigned a value of 1 (1200–9200 RNA copies/SFRS4 copy, Fig. 4C). The level of RNA decreased by nearly 30 % for 5UTR-H2AE-5BSL-3UTR$_{Kistem}$ and 5UTR-H2AE-5BSL-3UTR$_{TD}$ (73 ± 16 % and 72 ± 13 % of the wild type, respectively), indicating mutations that prevent RNA dimerization led to a slight decreased RNA half-life. Combined, our data indicate that reduced RNA stability can impact translation efficiency; however, this cannot completely explain the profound replication deficits observed.

Activity of the viral RdRp is dependent upon RNA dimerization

Because decreased translation efficiency cannot fully explain the replication phenotype of the SL2 mutants, we used long RNA templates to test whether or not these SL2 mutations were affecting RdRp activity. These RNA templates are 555 nt long and span the region upstream of the SL9110 sequence [5], and extend to the 3′ end of the genome (WT_{555}, Fig. 1A). RdRp-mediated RNA synthesis levels decreased significantly in the TD_{555} mutant (78 ± 4 %) compared with the wild type RNA (WT_{555}). RNA synthesis of the kistem$_{555}$ mutant was even lower (55 ± 3 %, Fig. 5), suggesting that this was a poorer template for the RdRp. To analyze whether 5BSL3.2/SL2 interaction is responsible for this decrease, we studied the role of this intra-molecular RNA interaction on RNA synthesis. Therefore, we used an RNA as a template that disrupted this interaction (5BSL3.2$_{555}$mut) and a template in which the interaction was restored (5BSL3.2$_{555}$-mut/SL2$_{555}$-mut). For both of them, the level of RNA synthesis was not affected compared with the WT_{555} RNA template (Fig. 5). These data show that the interaction between 5BSL3.2 and SL2 is not involved in RdRp-mediated RNA synthesis. Thus, our results indicate that the efficiency of negative strand RNA synthesis by RdRp, depends only on inter-molecular interactions that likely lead to the dimerization of two plus strands at the 3′ end of the viral genome.

Discussion

In this work, we describe the biological role of the SL2 stem-loop during HCV replication. By using viruses containing mutations within SL2, we show that the structural integrity of the SL2 bulge is necessary for efficient viral replication. Our data indicate that SL2 mutations neither significantly impair translation nor encapsidation but that SL2 integrity is essential for efficient RNA synthesis in vitro. Because disruption of 5BSL3.2/SL2 interaction had no effect on RNA synthesis (Fig. 5), we conclude that these intra-molecular RNA interactions already described [6, 7] do not hamper the RNA synthesis. In contrast, the inter-molecular interaction modified in the mutant TD_{555} and Kistem$_{555}$ play an active role in the RNA synthesis by RdRp. Together, these results support the hypothesis that genomic RNA replication is reduced when dimerization is impeded.

Twenty-four hours after transfection, GLuc expression from mutant viruses remained similar to that of the wild type virus (Fig. 3) indicating that translation was either not influenced at all or slightly influenced. These results were

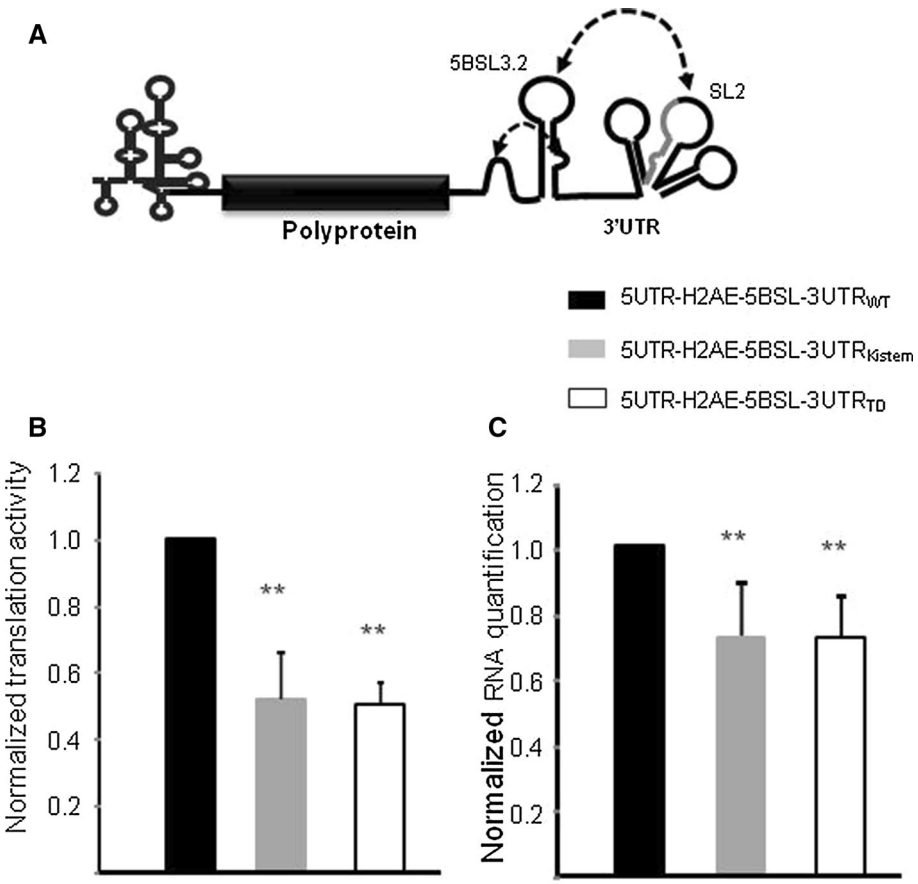

Fig. 4 The effect of SL2 bulge mutations on translation. **A** Schematic representation of the RNA constructs. Known RNA lon-range interactions are symbolized by *arrows*. **B** The RNA constructs 5UTR-H2AE-5BSL-3UTR$_{WT}$, 5UTR-H2AE-5BSL-3UTR$_{Kistem}$ and 5UTR-H2AE-5BSL-3UTR$_{TD}$ (300 ng) were transfected into 2×10^4 Huh7-QR cells plated in 96-well plates using DMRIE-C; the cells were recovered after 24 h of culture, and the mean fluorescence was measured using flow cytometry. The results were normalized to 1 based on the wild type construct ($n = 8$ independent experiments in triplicate/error bars, mean ± SEM using 3 different RNA preparations, *double asterisks*, $p < 0.01$ using Student t test). **c** One microgram of the RNA constructs 5UTR-H2AE-5BSL-3UTR$_{WT}$, 5UTR-H2AE-5BSL-3UTR$_{Kistem}$ and 5UTR-H2AE-5BSL-3UTR$_{TD}$ was transfected into 8×10^4 Huh7-QR cells that were plated the day before into 24 well plates using DMRIE-C. Twenty-four and seventy-two hours after transfection, RNAs were extracted using TRI-Reagent as described in the "Materials and methods". The RNA amount was quantified by RT-qPCR of the EGFP gene using SFRS4 RNA as a control. The results were expressed as the slope of RNA quantities between 72 and 24 h then normalized to 1 for the wild type construct ($n = 3$ independent experiments/*error bars*, mean ± SEM using 3 different RNA preparations, *double asterisks*, $p < 0.01$ using Student t test)

supported by experiments performed using monocistronic RNA for which a decrease in translation is correlated to RNA degradation (Fig. 4). However, in infected cells, the amount of RNA depends on the balance between RNA replication and RNA degradation making it impossible to conclude which of these stages is directly involved. Moreover, the presence of the membranous web or viral proteins could likely modify the RNA sensitivity to cellular RNAses. The observation that we report on naïve Huh7 cells (Fig. 4C) could not reflect the situation of infected cells. Thus, we cannot rule out the possibility that RNA stability is affected differently in infected cells than in naïve cells. Nevertheless, the 30 % decrease observed in translation cannot explain the dramatic decrease in infectivity of the mutated viral supernatant (Fig. 3B, plating 2). Thus, these results support the importance of SL2 structural integrity that likely lead to the dimerization of HCV genomic RNA in RNA replication.

Several groups have described dimerization of HCV genomic RNA. However, only Shetty et al. [17] studied dimerization in the context of viral replication. In their work, the authors did not discuss the importance of RNA dimerization for viral replication because only a weak effect on HCV replication and infectivity was observed when they introduced a UU mutation into the SL2 bulge (V3DLS_UU). Our results obtained using a non-denaturing gel (Fig. 2B) unambiguously showed that the UU mutation generated an RNA structure (SL2$_{UU}$) with a conformation

different from that of the other mutants. Then, $SL2_{UU}$ is probably not an appropriate model to investigate the effect of dimerization on HCV replication. However, even if the short RNA $SL2_{UU}$ was not able to self-associate in vitro (Fig. 2B), it cannot be excluded that the UU mutant can dimerize in cellulo. The $SL2_{kistem}$ mutant was designed as a stem-loop that impedes the structural dynamics that $SL2_{WT}$ undergoes between two conformations: one of them is able to interact with 5BSL3.2 through loop–loop interactions and the other one self-associates [15, 18]. The mutations inserted into the kistem mutant prevent this conformational equilibrium by generating a perfect stem-loop structure, as predicted by Mfold, observed on native gel and characterized kinetically by SPR [18]. Translocating the bulge of SL2 from the 5′ to the 3′ side of the stem (mutant TD) also prevented dimerization (Fig. 2A, e). Furthermore, the use of longer RNA templates (555 nt) with these mutations strongly impacted the RdRp activity, supporting the conclusion that inter-molecular RNA interactions triggered by the self-association of two SL2 structures are crucial for polymerase activity. This argues in favor of dimerization of the HCV genomic RNA.

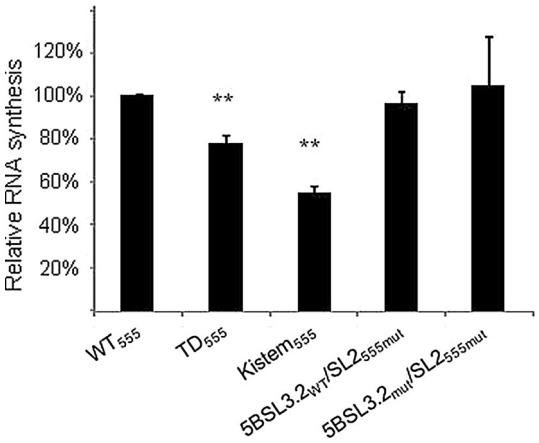

Fig. 5 Effect of SL2 bulge mutations on RNA synthesis. The RdRp assay was performed using purified NS5B (320 nM) and mutants RNAs as templates as described in the Materials and Methods section. Mutations of the SL2 bulge were introduced into SL2 ($Kistem_{555}$ and TD_{555}). Disruption of the 5BSL3.2/SL2 interaction was obtained by mutation of the SL2 apical loop ($SL2_{555mut}$), and restoration of the 5BSL3.2/SL2 interaction was obtained by introducing reciprocal mutations into the 5BSL3.2 apical loop ($5BSL3.2_{mut}/SL2_{555mut}$). RNA synthesis was determined after TCA precipitation and expressed as the percentage of the value obtained with the wild type RNA normalized to 100 ($n = 3$ to 5 independent experiments/error bars, mean ± SEM using 2 different RNA preparations, *double asterisks*, $p < 0.001$ using Student test)

Ten years ago, Cristofari et al. showed that the core protein promoted RNA dimerization. Since the replicon autonomously replicates in cell culture (in a mechanism similar to the virus) without core protein, this suggests that the core protein is not required for RNA synthesis but might actually regulate the level of RNA(−) molecule in the virus by increasing the recruitment of the viral polymerases discussed by these authors [13].

Dimerization of genomic RNA is now widely accepted for retroviridae such as for instance HIV-1, but for many decades this was not formally demonstrated in cell culture. The conclusion stating that dimerization is biologically relevant for retroviridae was drawn from in vitro experiments after disruption of viral particles [30, 31], from the existence of a strand transfer and identification of recombinants viruses in infected patients. This hypothesis was supported experimentally only in 2009. In this study, the authors pointed out that "A generally accepted but unproven assumption is that 1 dimer is encapsidated in each virion" [32]. We do not bring direct evidence that the genome of HCV dimerizes in cellulo. However, our data supported by other studies, strongly argue in favor of the dimerization of the HCV genomic RNA. Dimerization of the full genomic RNA has been indeed experimentally characterized by Tuplin [4] and Romero-Lopez [3]. Using SHAPE probing, both studies suggest the engagement of the 5′ part of the SL2 stem in an RNA dimer, while its 3′ part became single stranded Using J6/JFH-1 strain, Tuplin et al. ([4], Fig. 4) showed that the 5′ part of the SL2 stem (nt 9571-9582 in their paper) is almost not reactive particularly for nt 9574-9582 likely because it is involved either in dimerization or in the SL2 structure. On the

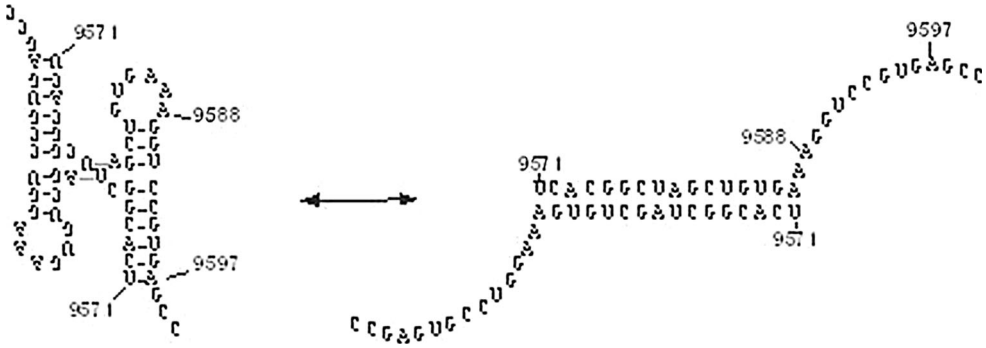

Fig. 6 Schematic of SL2 dimerization

contrary, the 3′ part of this stem (nt 9589-9597) is significantly more reactive (nt 9589-9597) because these nucleotides are not hybridized during dimerization. Romero-Lopez et al. also showed that the 3′part of the SL2 stem was accessible while the 5′ part was engaged in interactions. The authors showed indeed (Fig. 2A) that two DNA oligonucleotides 9543 and 9550 (reported in Fig. 2C) could interact with the 3′part of the SL2 stem, while two others, 9529 and 9536 could not bind to its 5′part. Both of these studies fit perfectly with the dimerization model proposed in Fig. 6 and argue strongly in favor of HCV genomic RNA dimerization.

For HIV, dimerization of genomic RNA leads to recombination events. The mechanisms, extensively investigated, involve jumps of the reverse transcriptase between the two dimerized plus strands. Numerous studies have established that packaging of the viral genome and retro-transcription depends on this dimerization stage in the *Retroviridae* family [10, 11]. In the case of HCV, several recombinant strains have been reported [19] and in vitro recombination events have been documented more recently [21]. Recombination would require the HCV RdRp to jump from one plus strand to another, which is only possible if the two strands are within close proximity to each other. Dimerization of genomic RNA could be an efficient mechanism for the virus to generate diversity by recombination.

In summary, this study demonstrates that genomic RNA dimerization is essential to the HCV life cycle, at least partly because the viral polymerase requires dimerization of the RNA template for efficient RNA synthesis. Dimerization occurs via the SL2 structure, which is perfectly conserved among the HCV genotypes, making SL2 a valuable target for the development of new HCV inhibitors. Additionally, our data provide the basis for a possible mechanism responsible for the presence of viral recombinants in HCV.

Acknowledgments We thank the structural biophysico-chemistry facility (UMS 3033/US001) of the Institut Européen de Chimie et Biologie (Pessac, France) for access to the Biacore T200 instrument that was acquired with the support of the Conseil Régional d'Aquitaine, the GIS-IBiSA, and the Cellule Hôtels à Projets of the CNRS. This work was supported by the Agence Nationale de Recherche contre le SIDA (ANRS), the Centre National de la Recherche Scientifique (CNRS), the Institut National de la Santé et de la Recherche Médicale (INSERM) and the Université de Bordeaux. The authors would like to thank Dr. Clint Smith for critical review of the manuscript.

References

1. Romero-López C (2014) Structure-function relationship in viral RNA genomes: the case of hepatitis C virus. World J Med Genet 4:6. doi:10.5496/wjmg.v4.i2.6
2. Diaz-Toledano R, Ariza-Mateos A, Birk A et al (2009) In vitro characterization of a miR-122-sensitive double-helical switch element in the 5′ region of hepatitis C virus RNA. Nucleic Acids Res. doi:10.1093/nar/gkp553
3. Romero-Lopez C, Barroso-delJesus A, Garcia-Sacristan A et al (2014) End-to-end crosstalk within the hepatitis C virus genome mediates the conformational switch of the 3′X-tail region. Nucleic Acids Res 42:567–582. doi:10.1093/nar/gkt841
4. Tuplin A, Struthers M, Simmonds P, Evans DJ (2012) A twist in the tail: SHAPE mapping of long-range interactions and structural rearrangements of RNA elements involved in HCV replication. Nucleic Acids Res. doi:10.1093/nar/gks370
5. Diviney S, Tuplin A, Struthers M et al (2008) A hepatitis C virus cis-acting replication element forms a long-range RNA-RNA interaction with upstream RNA sequences in NS5B. J Virol 82:9008–9022. doi:10.1128/JVI.02326-07
6. Friebe P, Boudet J, Simorre JP, Bartenschlager R (2005) Kissing-loop interaction in the 3′ end of the hepatitis C virus genome essential for RNA replication. J Virol 79:380–392
7. You S, Stump DD, Branch AD, Rice CM (2004) A cis-acting replication element in the sequence encoding the NS5B RNA-dependent RNA polymerase is required for hepatitis C Virus RNA replication. J Virol 78:1352–1366
8. Kim YK, Lee SH, KIM CS et al (2003) Long-range RNA–RNA interaction between the 5′ nontranslated region and the core-coding sequences of hepatitis C virus modulates the IRES-dependent translation. RNA 9:599–606
9. Romero-Lopez C, Diaz-Gonzalez R, Barroso-Deljesus A, Berzal-Herranz A (2009) Inhibition of HCV replication and IRES-dependent translation by an RNA molecule. J Gen Virol. doi:10.1099/vir.0.008821-0
10. Housset V, De Rocquigny H, Roques BP et al (1993) Basic amino acids flanking the zinc finger of Moloney murine leukemia virus nucleocapsid protein NCp10 are critical for virus infectivity. J Virol 67:2537–2545
11. Johnson SF, Telesnitsky A (2010) Retroviral RNA dimerization and packaging: the what, how, when, where, and why. PLoS Pathog 6:e1001007. doi:10.1371/journal.ppat.1001007
12. Ishimaru D, Plant EP, Sims AC et al (2013) RNA dimerization plays a role in ribosomal frameshifting of the SARS coronavirus. Nucleic Acids Res 41:2594–2608. doi:10.1093/nar/gks1361
13. Cristofari G, Ivanyi-Nagy R, Gabus C et al (2004) The hepatitis C virus core protein is a potent nucleic acid chaperone that directs dimerization of the viral (+) strand RNA in vitro. Nucl Acids Res 32:2623–2631
14. Sharma KK, de Rocquigny H, Darlix JL et al (2012) Analysis of the RNA chaperoning activity of the hepatitis C virus core protein on the conserved 3′X region of the viral genome. Nucleic Acids Res 40:2540–2553. doi:10.1093/nar/gkr1140
15. Shetty S, Stefanovic S, Mihailescu MR (2012) Hepatitis C virus RNA: molecular switches mediated by long-range RNA–RNA interactions? Nucleic Acids Res. doi:10.1093/nar/gks1318
16. Ivanyi-Nagy R, Kanevsky I, Gabus C et al (2006) Analysis of hepatitis C virus RNA dimerization and core-RNA interactions. Nucleic Acids Res 34:2618–2633
17. Shetty S, Kim S, Shimakami T et al (2010) Hepatitis C virus genomic RNA dimerization is mediated via a kissing complex intermediate. RNA 16:913–925
18. Palau W, Masante C, Ventura M, Di Primo C (2013) Direct evidence for RNA–RNA interactions at the 3′ end of the Hepatitis C virus genome using surface plasmon resonance. RNA. doi:10.1261/rna.037606.112
19. Morel V, Fournier C, François C et al (2011) Genetic recombination of the hepatitis C virus: clinical implications. J Viral Hepat 18:77–83. doi:10.1111/j.1365-2893.2010.01367.x

20. Galli A, Bukh J (2014) Comparative analysis of the molecular mechanisms of recombination in hepatitis C virus. Trends Microbiol. doi:10.1016/j.tim.2014.02.005
21. Scheel TKH, Galli A, Li Y-P et al (2013) Productive homologous and non-homologous recombination of hepatitis C virus in cell culture. PLoS Pathog 9:e1003228. doi:10.1371/journal.ppat.1003228
22. González-Candelas F, López-Labrador FX, Bracho MA (2011) Recombination in hepatitis C Virus. Viruses 3:2006–2024. doi:10.3390/v3102006
23. Zuker M (2003) Mfold web server for nucleic acid folding and hybridization prediction. Nucleic Acids Res 38:3406–3415
24. Dumas E, Masante C, Astier-Gin T et al (2007) The hepatitis C virus minigenome: a new cellular model for studying viral replication. J Virol Methods 142:59–66
25. Bitard J, Chognard G, Dumas E et al (2010) Hijacking hepatitis C viral replication with a non-coding replicative RNA. Antivir Res 87:9–15
26. Di Primo C, Dausse E, Toulmé J-J (2011) Surface plasmon resonance investigation of RNA aptamer–RNA ligand interactions. In: Goodchild J (ed) Therapeutic oligonucleotides. Humana Press, New York, pp 279–300
27. Waxman S, Wurmbach E (2007) De-regulation of common housekeeping genes in hepatocellular carcinoma. BMC Genom 8:243
28. Astier-Gin T, Bellecave P, Litvak S, Ventura M (2005) Template requirements and binding of hepatitis C virus NS5B polymerase during in vitro RNA synthesis from the 3′-end of virus minus-strand RNA. FEBS J 272:3872–3886
29. Mahias K, Ahmed-El-Sayed N, Masante C et al (2010) Identification of a structural element of the hepatitis C virus minus strand RNA involved in the initiation of RNA synthesis. Nucleic Acids Res 38:4079–4091
30. Bender W, Davidson N (1976) Mapping of poly(A) sequences in the electron microscope reveals unusual structure of type C oncornavirus RNA molecules. Cell 7:595–607
31. Mujeeb A, Clever JL, Billeci TM et al (1998) Structure of the dimer initiation complex of HIV-1 genomic RNA. Nat Struct Biol 5:432–436
32. Chen J, Nikolaitchik O, Singh J et al (2009) High efficiency of HIV-1 genomic RNA packaging and heterozygote formation revealed by single virion analysis. Proc Natl Acad Sci 106:13535–13540. doi:10.1073/pnas.0906822106